CHEMISTRY
A EUROPEAN JOURNAL

Polyoxometalate-Supported Y– and Yb^{III}–Hydroxo/Oxo Clusters from Carbonate-Assisted Hydrolysis

Xikui Fang,[a] Travis M. Anderson,[a] Cristiano Benelli,[b] and Craig L. Hill*[a]

In memory of Professor Jingfu Liu

Abstract: Carbonate-assisted hydrolysis of Y or Yb^{III} ions in the presence of the trivacant Wells–Dawson polyoxoanion, α-$[P_2W_{15}O_{56}]^{12-}$, produced two polyoxometalate-supported Y– or Yb^{III}–hydroxo/oxo clusters, which have been characterized by single-crystal X-ray structure determination. The structure of the Y complex consists of a distorted $Y_4(OH)_4$ cubane cluster encapsulated by two lacunary α-$[P_2W_{15}O_{56}]^{12-}$ units, while the Yb cluster features a hexametallic core centered around a μ_6-oxo atom with each Yb_3^{III} triangular face capped by an oxo or a hydroxo group. Magnetization measurements of the ytterbium(III) derivative suggested that intermolecular dipolar exchange is present at low temperatures (below 15 K). Despite its absence in the structures themselves, control experiments show that carbonate not only functions in the hydrolysis, it also influences the structure of the complexes by complexation to yttrium and the f-block elements.

Keywords: carbonate · cluster compounds · lanthanides · polyoxometalates · self-assembly

Introduction

The rational self-assembly of modular and multicomponent systems into larger structures or materials with useful properties continues to be as important technologically as it is challenging to achieve. In this context, the formation of lanthanide–hydroxo/oxo clusters with noteworthy spectroscopic, magnetic, and catalytic properties is of interest.[1] Current efforts to synthesize new Ln–hydroxo/oxo clusters (Ln = lanthanide) are stimulated by the potential to develop synthetic nucleases for the hydrolysis of phosphate diester bonds, including the robust bonds of nucleic acids.[2] A common approach for the synthesis of such complexes is to utilize chelating ligands such as amino acids, ketonates, carboxylates, and alkoxides to control the hydrolysis of the metal ions.[3] The choice of bridging ligand(s) is critical in that the ligands not only provide appropriate electron-donor character and symmetry, they also stabilize the cluster by electrostatically or sterically counteracting the tendency for further aggregation. On the other hand, the Ln^{III} and Y ions generally display large and variable coordination numbers (CN = 8–12) and show minimal stereochemical preferences due to the small energy differences associated with the various coordination geometries.[4] This makes it difficult to control the coordination environment of the Ln^{III} centers and therefore impedes fine-tuning of the electronic, spectroscopic, and magnetic properties of such clusters. As a result, a crucial but challenging step towards rational design lies in selective incorporation of Ln^{III} ions into these highly organized architectures with the assistance of highly predisposed ligands.

Herein we report two such hydroxo/oxo clusters supported by the multidentate polyoxotungstate ligand, α-$[P_2W_{15}O_{56}]^{12-}$, derived from the parent Wells–Dawson α-$[P_2W_{18}O_{62}]^{6-}$ by controlled base degradation. The trivacant complex, α-$[P_2W_{15}O_{56}]^{12-}$, has seven terminal oxo groups in the M_3 (or "cap"; M = metal ion) region produced by base-associated hydrolysis, which can be readily used for metal ion coordination. However, the incorporation of metal ions into all three vacant sites has been limited to the first two rows of transition metals to date except for a uranium polyoxometalate (POM) recently reported by Pope et al., $[(UO_2)_{12}(\mu_3\text{-}O)_4(\mu_2\text{-}H_2O)_{12}(P_2W_{15}O_{56})_4]^{32-}$.[5] Representative

[a] X. Fang, Dr. T. M. Anderson, Prof. C. L. Hill
Department of Chemistry, Emory University
1515 Dickey Drive, Atlanta, GA 30322 (USA)
Fax: (+1) 404-727-6076
E-mail: chill@emory.edu

[b] Prof. C. Benelli
Department of Chemistry
Scientific Campus of the University of Florence
Via della Lastrucci 3, 50019 Sesto Fiorentino
Florence (Italy)

DOI: 10.1002/chem.200400774

examples of metal incorporation into α-$[P_2W_{15}O_{56}]^{12-/16-}$ include $[P_4W_{30}M_4O_{112}]^{16-}$ (M = Co^{II}, Cu^{II}, Zn^{II}, Mn^{II}, or Fe^{III}),[6–10] a di-iron(III)-substituted analogue $[Fe_2(NaOH_2)_2(P_2W_{15}O_{56})_2]^{16-}$,[11] $[P_2W_{15}M_3O_{62}]^{9-}$ (M = V or Nb),[12–15] a polyoxothiometalate $[(H_2P_2W_{15}O_{56})_4\{Mo_2O_2S_2(H_2O)_2\}_4\{Mo_4S_4O_4(OH)_2(H_2O)\}_2]^{12-}$,[16] and recently reported Ti complexes (dimeric $[TiP_2W_{15}O_{55}OH]_2^{14-}$, tetrameric $[Ti_3P_2W_{15}O_{57.5}(OH)_3]_4^{24-}$ and $[(P_2W_{15}Ti_3O_{60.5})_4]^{36-}$).[17] This work represents the first example of the incorporation of lanthanide ions into the trivacant Wells–Dawson-type polyanion system. The unusual stabilization forces observed for the bridging hydroxo/oxo moieties further distinguish these new complexes from the examples above.

Results and Discussion

Synthesis and characterization: The two new POM-supported hydroxo/oxo clusters, $[\{Y_4(\mu_3\text{-}OH)_4(H_2O)_8\}(\alpha\text{-}P_2W_{15}O_{56})_2]^{16-}$ (**1**) and $[\{Yb_6(\mu_6\text{-}O)(\mu_3\text{-}OH)_6(H_2O)_6\}(\alpha\text{-}P_2W_{15}O_{56})_2]^{14-}$ (**2**), were prepared from controlled hydrolysis in aqueous solutions. The reaction of α-$[P_2W_{15}O_{56}]^{12-}$ with YCl_3 or $Yb(NO_3)_3$ in an aqueous Na_2CO_3 solution (0.1 M) afforded a slurry, from which **1** and **2** were obtained in 22.8 and 35.2 % yields, respectively, after recrystallization. Both complexes have been characterized by ^{31}P NMR and IR spectroscopy, and the solid-state structures of **1** and **2** were established by elemental analysis and single-crystal X-ray diffraction. Carbonate not only functions as a hydrolysis reagent and buffer in which the lacunary polyoxoanion is relatively stabilized, it also facilitates the formation of a wide range of bridging hydroxo units which fortify the lanthanide–hydroxo/oxo cluster framework.

The structure of **1** is composed of two α-$[P_2W_{15}O_{56}]^{12-}$ ligands encapsulating a central tetranuclear $[Y_4(OH)_4]^{8+}$ unit (Figure 1a). Bond valence sum (BVS) calculations unequivocally establish that all four μ_3-bridging oxygen atoms are monoprotonated (BVS ~ 1.2; Table 1).[18] In the polycationic $[Y_4(OH)_4]^{8+}$ unit, the four Y^{III} ions are linked by the μ_3-OH bridges to form a highly distorted cubane-like core, elongated along the direction of the four phosphorus atoms, with two short and four long Y–Y contacts of 3.482 and 3.845 Å, respectively (Figure 1b). The molecule appears to be centrosymmetric because the central hydroxo–lanthanide core is disordered over two equally weighted orientations in the crystal, which are related by the crystallographic inversion center. There are two distinct yttrium sites in **1** for each orientation, both of which have a triangularly distorted dodecahedral geometry. Three triply bridging hydroxo groups, two oxygen atoms from two different WO_6 octahedra, one oxygen atom from a PO_4 tetrahedron, and two terminal aqua ligands complete each coordination sphere. The Y1 and Y4 atoms are ligated by two oxygen atoms from two edge-sharing WO_6 octahedra, while two corner-sharing WO_6 octahedra on the opposite side of the same hexa-tungsten belt serve as the linking groups for Y2 and Y3 (Figure 1). Thus, anion **1** has approximate C_2 symmetry with the two-fold axis bisecting the Y1-Y4 and Y2-Y3 vectors. The ^{31}P NMR spectra of **1** shows two peaks at −3.65 and −14.00 ppm (Figure 2) for the two pairs of proximal and distal P atoms, respectively, in the two α-$[P_2W_{15}O_{56}]^{12-}$ units, consistent with the X-ray structure analysis. Finally we note that for each α-$[P_2W_{15}O_{56}]^{12-}$ unit, there are still two terminal W=O groups on the trivacant face that remain unassociated and therefore may serve as vacant coordination sites for further structure derivatization.

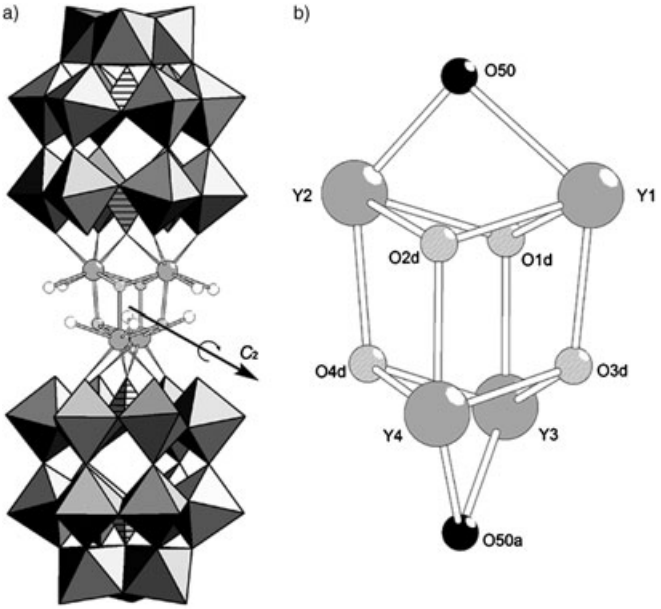

Figure 1. a) Complex **1** with the $[Y_4(\mu_3\text{-}OH)_4(H_2O)_8]^{8+}$ cubane cluster shown in ball-and-stick representation (Y, large gray spheres; OH, small hatched spheres; H_2O, small white spheres) with the top and bottom faces capped by two α-$[P_2W_{15}O_{56}]^{12-}$ trivacant POM units shown in polyhedral representation (WO_6 octahedra, gray; central PO_4 tetrahedra, hatched). The alternative positions of the disordered O and Y atoms are not shown. b) A perspective view of the Y_4 core showing all of the bridging oxygen atoms; the aqua ligands have been omitted for clarity (μ_2-bridging oxo, small black spheres).

Table 1. Bond valence sum (BVS) analysis for selected metal centers and oxygen sites in **1** and **2**.

Complex	Metal center	BVS[a]	Assigned oxidation state	Oxygen atom	BVS[a]	Assigned protonation state
1				μ_3-O1d	1.22	OH
				μ_3-O2d	1.29	OH
				μ_3-O3d	1.19	OH
				μ_3-O4d	1.20	OH
				μ_2-O50	2.17	O
2[b]	Yb1	3.03	+3	μ_3-O56	1.87	O
	Yb2	2.97	+3	μ_3-O57	1.21	OH
	Yb3	2.99	+3	μ_3-O58	1.27	OH
				μ_3-O59	1.17	OH
				μ_6-O60	1.57	O

[a] Values calculated using the method of I. D. Brown, ref. [18]. [b] There are three ytterbium sites in the asymmetric unit.

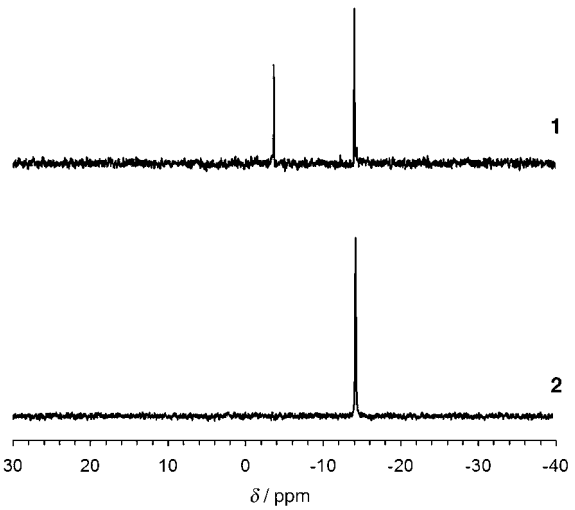

Figure 2. ^{31}P NMR of the sodium salts of **1** and **2** (0.01 mol L^{-1} in D_2O; referenced to 85% H_3PO_4).

The isolation of **1** firmly establishes that the cubane-like $Ln_4(\mu_3\text{-}OH)_4$ unit, like those observed in organolanthanide chemistry,[3] can function as a structural building block for larger complexes. It also shows the versatility of the α-$[P_2W_{15}O_{56}]^{12-}$ ligand as previous sandwich-type complexes ($[M_4(H_2O)_2(\alpha\text{-}P_2W_{15}O_{56})_2]^{12-/16-}$)[6–10] have four d-block metal ions (M) encapsulated between the two α-$[P_2W_{15}O_{56}]^{12-}$ units in a planar fashion. In addition, the formation of **2** from the hydrolytic reaction of Yb^{III} further illustrates the versatility of this ligand as three Yb^{III} cations now occupy the "holes" left by the three significantly smaller W^{VI} cations.[19] Once again, the hydroxo/oxo bridges play an essential role in stabilizing the framework of **2**.

The structure of **2** is composed of two α-$[P_2W_{15}O_{56}]^{12-}$ units bridged by a $[Yb_6(\mu_6\text{-}O)(\mu_3\text{-}OH)_6(H_2O)_6]^{10+}$ cluster. This Yb^{III}–hydroxo/oxo unit contains a central μ_6-oxygen atom (O60) in an M_6 octahedral coordination environment. Each Yb^{III}_3 triangular face is further capped by a μ_3-oxygen atom (Figure 3). Bond valence sum calculations were used to determine the oxidation state of the Yb centers and the protonation state of the bridging oxygen atoms (Table 1). Like those in **1**, all μ_3-bridging oxygen atoms were determined to be hydroxo groups except for the two on the top and bottom faces (O56 and O56a), which are terminal oxygen atoms from the PO_4 tetrahedra and remain unprotonated (Table 1). Although we assign the central μ_6-O atom (O60) as oxo, its calculated BVS value (1.57) lies between that for an ideal hydroxo (~1.2) and oxo (~2.0) atom. This more likely reflects the unusual M_6 coordination environment and the commensurately less defensible BVS calculation than partial protonation. A similar hexa-metal core was reported in a cyanide-bridged chain polymer, $[\{Yb_6(\mu_6\text{-}O)(\mu_3\text{-}OH)_8(dmf)_{16}(\mu\text{-}CN)Pd(\mu\text{-}CN)(CN)_2\}^6]_n$ (**3**).[20] However, in **2** the two faces used for linking the POM ligands are capped by the terminal oxo groups (P=O) of the α-$[P_2W_{15}O_{56}]^{12-}$ units instead of hydroxo groups in **3**, suggesting a specific role for the POM units in the formation and/or stabilization of the central Yb_6 core. The structure of **2** exhibits D_{3d} symmetry, with each C_2 axis perpendicular to one of the three mirror planes containing the main C_3 axis (Figure 3a).

The ^{31}P NMR spectrum of **2** exhibits only one rather sharp peak at −14.2 ppm ($\Delta\nu_{1/2}$ = 19.4 Hz), which is attributed to the two distal P atoms (Figure 2). The signal for the two proximal phosphorus atoms are too broadened for detection, due to the close proximity of these phosphorus atoms to the paramagnetic Yb^{III} centers. This is rarely seen in ytterbium(III)-substituted polyoxoanion complexes. In most cases, the interaction between the unpaired electrons from Yb^{III} and the nuclear spin of the phosphorus atoms often leads to broad but still observable signals.[21] On the other hand, the two distal phosphorus atoms are not strongly affected, as seen from their sharp peak and minor shift

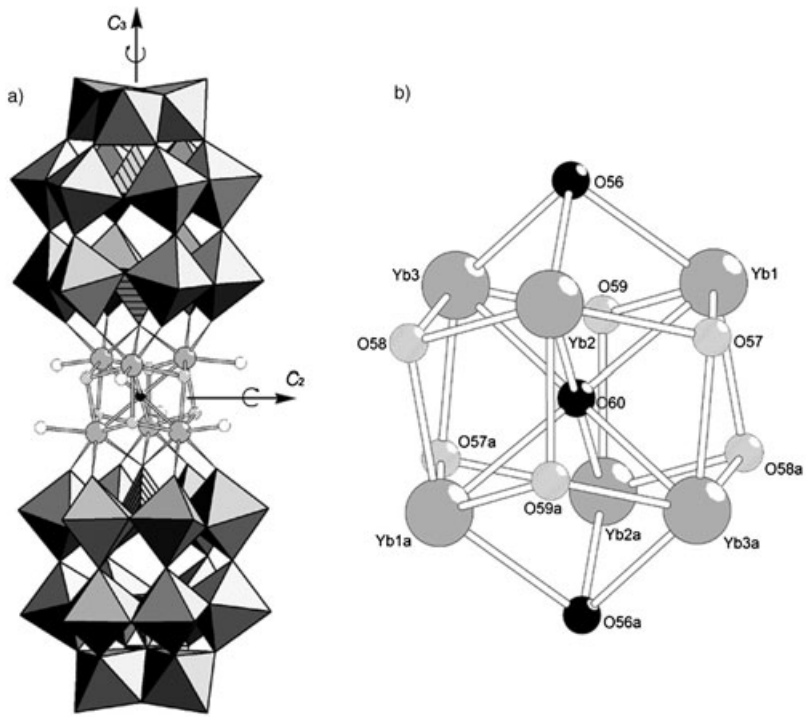

Figure 3. a) The structure of **2** (WO_6 octahedra, gray; central PO_4 tetrahedra, hatched; Yb, large gray spheres; OH, small hatched spheres; H_2O, small white spheres). b) The central hexanuclear $[Yb_6(\mu_6\text{-}O)(\mu_3\text{-}OH)_6(\mu_3\text{-}O)_2]^{6+}$ unit of **2**; the aqua ligands have been omitted for clarity (μ_3- and μ_6-bridging oxo, small black spheres).

from their diamagnetic positions (−14.00 ppm for **1** and −13.8 ppm for α-$[P_2W_{15}O_{56}]^{12-}$).[22]

A noteworthy solid-state structural feature of **2** (in a mixed $(CH_3)_2NH_2^+$ and NH_4^+ salt) is that the individual molecules are interlaced with each other in a manner that generates small one-dimensional tunnels along the crystallographic *c* axis (Figure 4). However, BET measurements with N_2 sorption/desorption show this crystalline material has a very low surface area ($<2\,m^2g^{-1}$). This can be attributed either to the small dimensions of the tunnel or to the presence of hydrogen bonding with the $(CH_3)_2NH_2^+$ and NH_4^+ cations proximal to the POM units.

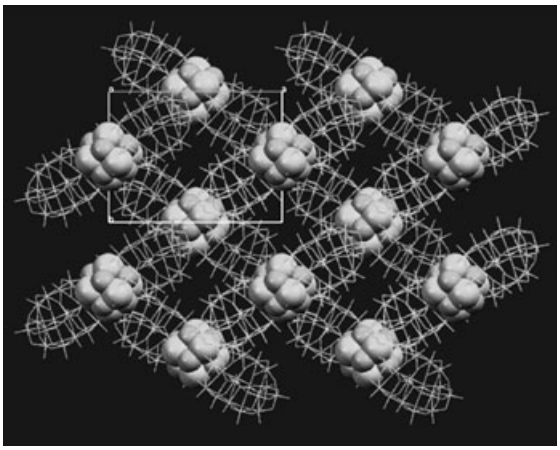

Figure 4. Packing diagram of **2** visualized along the crystallographic *c* axis. The countercations and the solvent H_2O molecules have been omitted for clarity; the polyoxoanion ligands are shown in wireframe notation whereas the central Yb-based cores are in space-filling notation.

Magnetic studies: The temperature dependence of the magnetic susceptibility of compound **2** is shown in Figure 5 in the form of a χT versus T plot (χ = molar magnetic susceptibility, T = temperature). At 300 K, χT is equal to 14.25 $cm^3\,mol^{-1}\,K$ which is the value expected for six magnetically insulated Yb^{III} ions ($6\times2.57\,cm^3\,mol^{-1}\,K$) in the $^2F_{7/2}$ ground state. The magnetic data have been analyzed by using a classical crystal-field approach: the temperature dependence of the magnetic susceptibility has been fitted assuming a local C_{2v} symmetry in the coordination sphere of each Yb ion. The best-fit parameters B_q^k are $B_0^2=499.5$, $B_2^2=686.4$, $B_0^4=-155.2$, $B_2^4=414.6$, $B_4^4=106.3$, $B_0^6=-15.3$, $B_2^6=140.7$, $B_4^6=105.0$, $B_6^6=-103.4\,cm^{-1}$, which have a splitting of the Kramers' doublets in the $^2F_{7/2}$ ground multiplet of 226, 662, and 928 cm^{-1} with respect to the ground state and are all well inside the range of reported splittings.[23,24] The fit nicely reproduces the experimental pattern from room temperature down to approximately 10 K. Below this temperature the observed susceptibilities are lower than the calculated ones. The discrepancies observed in the low temperature region may be due to some kind of magnetic interaction between the Yb^{III} ions. The analysis of the magnetic interactions for this ion are made more complex by the presence of an orbital contribution in its ground state that prevents the use of an isotropic Heisenberg–Dirac–Van Vleck (HDVV) Hamiltonian. Since the presence of a superexchange mechanism can be ruled out, the magnetic interaction can be due to either an intracluster and/or an intercluster dipolar exchange. It could be possible to treat the intracluster dipolar interaction in an analytical way.[25] However, the complexity of this cluster (6 ions involving at least 12 different interactions) makes the calculation very difficult because of the total number of involved states. It is possible to calculate the influence of the dipolar intramolecular interaction by making some approximations. Due to the energy separation of the three Kramers doublets, the magnetic behavior in the low-temperature region could be due only to the doublet with the lowest energy, as at 15 K the highest energy levels are substantially depopulated. It is therefore possible to treat the low-energy doublet with a fictitious spin of $^1/_2$ and an effective *g* factor. The second approximation is to consider the intramolecular dipolar interaction as isotropic. This means that in any case the calculations are indicative of the presence of this kind of exchange mechanism, but the procedure does not give any fully reliable parameters. On the other hand, the intermolecular dipolar exchange has been taken into account with the classical mean-field approach.

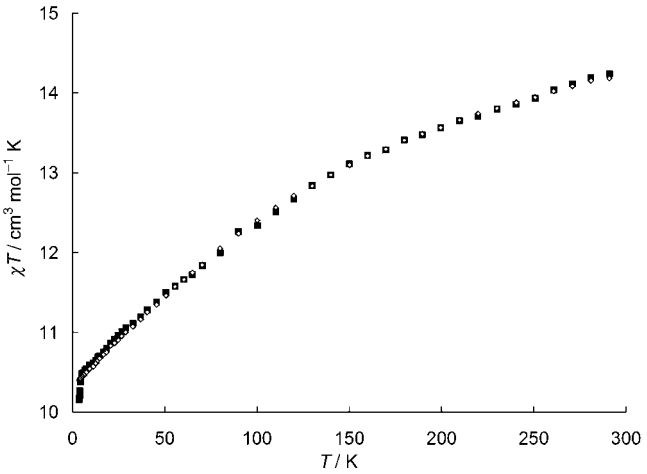

Figure 5. Temperature dependence of the χT values in the 300–1.5 K temperature range for **2**: experimental (■) and calculated values (◇).

The intramolecular-exchange coupling constant was fixed to the value calculated according to the mean Yb–Yb distances observed in the crystal structure. All attempts to reproduce the low-temperature pattern with the intramolecular interaction were unsuccessful, while the calculation based on the intermolecular approach gave interesting results as shown in Figure 6. The values used to calculate the curve were $g=1.8$, with an intermolecular interaction value of $\sim0.01\,cm^{-1}$. It is possible to conclude that the magnetic behavior of the Yb_6 cluster can be described on the basis of the thermal depopulation within the ground multiplet from room temperature down to 15 K. Below this temperature

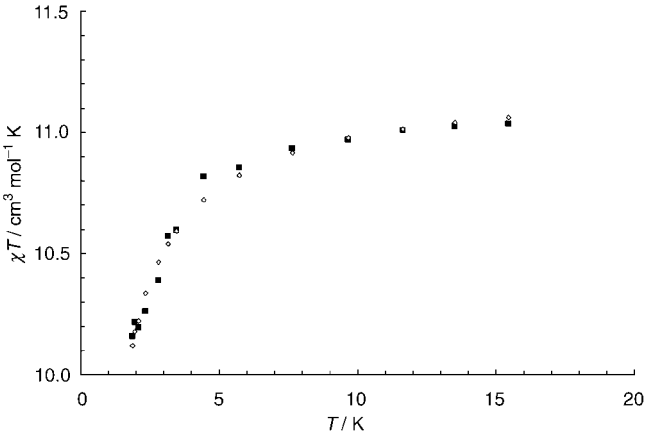

Figure 6. Temperature dependence of the χT values in the 15–1.5 K temperature range for **2**: experimental (■) and calculated values (◇).

the magnetic behavior is described by an intermolecular exchange which is operative between the different clusters.

The role(s) of carbonate: One of the goals of this work was to determine what kind of role(s) the carbonate is playing in the formation of lanthanide (especially late-group lanthanide) complexes with polyoxoanions. Carbonate has not been previously used in the preparations of lanthanide–hydroxo clusters, most likely because the carbonate salts have low solubility and are not easily displaced by other ligands. Generally, finite-sized lanthanide–hydroxo complexes are isolated with the use of N-containing supporting ligands.[3] These ligands contribute to the higher water solubility of the lanthanide complexes in part because of the additional hydrogen-bonding interactions involving the N atom(s).[1a] The nucleophilic environment afforded by the α-$[P_2W_{15}O_{56}]^{12-}$ anion at its vacant sites may inhibit carbonate from entering the coordination sphere of the Ln ions, in contrast to the situation previously described in which carbonate has a stronger coordinating ability than the supporting ligands. However, several lines of evidence suggest that the self-assembly of **1** and **2** is at least partly influenced by the pre-coordination of carbonate to the Ln ions.[26] First, it is well known that carbonate can play an important role in the environmental fate of f-block metal ions due to its strong and facile coordination to these metals.[27] We recently reported a carbonate-encapsulated sandwich compound in which strong bonds to carbonate actually stabilize the structure.[28] Carbonate appears to play a role in the formation of **1** and **2** even in the presence of the nucleophilic polyoxoanion ligands. Second, control experiments using NaOH at an adjusted comparable pH as the hydrolysis reagent afforded compounds with completely different structures from those seen in **1** and **2**.[29] This suggests that the carbonate ligand is critical to the formation of the hydroxo–lanthanide-cluster core (perhaps as a templating agent) and is not just a hydrolysis reagent.

Conclusion

We present a new carbonate-assisted hydrolysis route to lanthanide–hydroxo/oxo clusters. These new structural families illustrate that this particular polyoxoanion ligand is quite versatile in supporting lanthanide clusters and stabilizing them. Although it is still not entirely clear what structural function(s) carbonate has in these reactions, given the wide range of lacunary POMs that can be employed as ligands for cationic clusters, we anticipate this general methodology may lead to the preparation of many new hydroxo–lanthanide cluster complexes.

Experimental Section

All reagents and metal salts were used as obtained from Aldrich. The polyoxotungstate ligand $Na_{12}[\alpha\text{-}P_2W_{15}O_{56}]\cdot 18H_2O$ was prepared according to the literature method.[22]

$Na_{16}[\{Y_4(\mu_3\text{-}OH)_4(H_2O)_8\}(\alpha\text{-}P_2W_{15}O_{56})_2]\cdot 42H_2O$ (Na1): A sample of $YCl_3\cdot 6H_2O$ (0.28 g, 0.92 mmol) was dissolved in water (10 mL) and aqueous Na_2CO_3 (1 M, 1 mL) was added with stirring. Solid $Na_{12}[\alpha\text{-}P_2W_{15}O_{56}]\cdot 18H_2O$ (1.00 g, 0.23 mmol) was then added to the mixture in small portions over a period of 20 min with vigorous stirring. After stirring for another 60 min, the solution was heated to 60 °C for 30 min and then cooled to room temperature. Any insoluble material present was removed by centrifugation. Solid NaCl (1.5 g) was added to the solution slowly and the mixture was cooled in an ice–water bath. After several hours, the slightly oily precipitate was separated and washed with ethanol (5 mL). The solid was then dried under suction. The crude product was dissolved in 5 mL of hot water and the solution was saturated with NaCl (~0.1 g). After cooling at 5 °C for several days, colorless crystals (0.24 g) were manually separated from the residual oily solid (yield 22.8 %). Diffraction-quality crystals were obtained by recrystallization from a dilute NaCl solution. Attempts to scale-up the reaction were unsuccessful, producing only an oily mixture of the target product and some unknown by-product(s). ^{31}P NMR (0.01 mol L^{-1} in D_2O; referenced to 85 % H_3PO_4): $\delta = -3.65$ ($\Delta\nu_{1/2} = 8.5$ Hz) and -14.00 ppm ($\Delta\nu_{1/2} = 7.6$ Hz); IR (KBr): $\tilde{\nu} =$ 1083 (s), 1028 (m), 940 (s), 925 (s), 907 (s), 878 (s), 817 (vs), 726 cm^{-1} (vs); elemental analysis calcd (%) for $H_{20}Na_{16}O_{124}P_4W_{30}Y_4\cdot 42H_2O$: Na 4.03, P 1.36, W 60.5, Y 3.90; found: Na 4.10, P 1.33, W 59.9, Y 3.93.

$Na_{14}[\{Yb_6(\mu_6\text{-}O)(\mu_3\text{-}OH)_6(H_2O)_6\}(\alpha\text{-}P_2W_{15}O_{56})_2]\cdot 45H_2O$ (Na2): A sample of $Yb(NO_3)_3\cdot 5H_2O$ (0.42 g, 0.94 mmol) was dissolved in water (10 mL) and aqueous Na_2CO_3 (1 M, 1 mL) was added with stirring. The slurry was heated to 80 °C and then solid $Na_{12}[\alpha\text{-}P_2W_{15}O_{56}]\cdot 18H_2O$ (1.00 g, 0.23 mmol) was added in small portions over a period of 20 min with vigorous stirring. The solution was maintained at 80 °C for 30 min and then cooled to room temperature. Any insoluble material present was removed by centrifugation. The solution was placed in an ice–water bath, solid NaCl (1.5 g) was added and the precipitate was collected by suction filtration on a medium frit. The crude product was dissolved in hot water (10 mL). The solution was then saturated with NaCl (~0.3 g) and cooled to 5 °C. This recrystallization procedure was repeated twice until a pure product was obtained (yield 35.2 %). ^{31}P NMR (0.01 mol L^{-1} in D_2O; referenced to 85 % H_3PO_4): $\delta = -14.20$ ppm ($\Delta\nu_{1/2} = 19.4$ Hz); IR (KBr): $\tilde{\nu} =$ 1088 (s), 1050 (m), 1014 (w), 998 (w, sh), 938 (vs), 905 (vs), 820 (vs), 726 cm^{-1} (vs); elemental analysis calcd (%) for $H_{18}Na_{14}O_{125}P_4W_{30}Yb_6\cdot 45H_2O$: Na 3.27, P 1.26, W 56.1, Yb 10.56; found: Na 3.32, P 1.23, W 55.9, Yb 10.63. Due to the solubility problems, diffraction-quality crystals were obtained as a mixed salt of $(CH_3)_2NH_2^+$ and NH_4^+. First, the sodium salt was converted to the ammonium salt by adding NH_4Cl to an aqueous solution of **Na2**. The precipitate was collected in a sintered-glass filter funnel and thoroughly dried in air. Then the ammonium salt (1.0 g) was dissolved in warm H_2O (15 mL) upon the addition of a small amount of $(CH_3)_2NH_2Cl$. Slow evaporation of the above solution at room temper-

ature resulted in diffraction-quality crystals in 2 days. IR and ^{31}P NMR spectroscopy confirmed that the structure of **2** is maintained after the ion exchange and recrystallization steps.

X-ray crystallographic structure determination: Crystal data collection and refinement parameters for **1** and **2** are given in Table 2. Suitable crystals were coated with Paratone N oil, suspended on a small fiber loop, and placed in a cooled nitrogen stream at 173 K on a Bruker D8 SMART APEX CCD sealed-tube diffractometer with graphite-monochromated $Mo_{K\alpha}$ (0.71073 Å) radiation. A sphere of data was measured using a series of combinations of φ and ω scans with 10 s frame exposures and 0.3° frame widths. Data collection, indexing, and initial cell refinements were all handled using SMART software.[30] Frame integration and final cell refinements were carried out using SAINT software.[31] The final cell parameters were determined from least-squares refinement on 9540 and 7965 reflections for **1** and **2**, respectively. The SADABS program was used to carry out absorption corrections.[32] The structure was solved using Direct Methods and difference Fourier techniques (SHELXTL, V6.12).[33] All metal atoms were refined anisotropically. Scattering factors and anomalous dispersion corrections were taken from the International Tables for X-ray Crystallography.[34] Structure solution, refinement, and generation of publication materials were performed by using SHELXTL, V6.12 software.[33]

Table 2. Crystallographic data and structure-refinement parameters for $Na_{16}[\{Y_4(\mu_3\text{-}OH)_4(H_2O)_8\}(\alpha\text{-}P_2W_{15}O_{56})_2]\cdot 42\,H_2O$ (**Na1**) and $[(CH_3)_2NH_2]_8(NH_4)_6[\{Yb_6(\mu_6\text{-}O)(\mu_3\text{-}OH)_6(H_2O)_6\}(\alpha\text{-}P_2W_{15}O_{56})_2]\cdot 34\,H_2O$ (**DMA,NH$_4$2**).

	Na1	**DMA,NH$_4$2**
formula	$H_{104}Na_{16}O_{166}P_4W_{30}Y_4$	$C_{16}H_{174}N_{14}O_{159}P_4W_{30}Yb_6$
M_r [g mol^{-1}]	9123.6	9785.2
crystal system	triclinic	monoclinic
space group	$P\bar{1}$	$P2_1/n$
a [Å]	12.831(1)	22.822(2)
b [Å]	14.970(1)	16.172(1)
c [Å]	21.702(2)	26.074(2)
α [°]	79.230(2)	90
β [°]	89.227(2)	111.341(2)
γ [°]	86.510(2)	90
V [Å^3]	4087.4(6)	8963.8(14)
T [K]	173(2)	173(2)
Z	1	2
ρ_{calcd} [Mg m^{-3}]	3.541	3.427
crystal size [mm]	0.14×0.10×0.08	0.25×0.06×0.04
μ [mm^{-1}]	22.568	22.379
$2\theta_{max}$	54.00	49.42
data/restraints/parameter	17842/0/585	15266/0/504
absorption correction	SADABS	SADABS
$R1/wR2$	0.0741/0.1646	0.0846/0.1737
goodness of fit	1.080	1.105
largest residuals [e Å^3]	+5.299/−6.396	+3.792/−2.272

Complex **1** crystallizes in space group $P\bar{1}$ making the molecule appear to be centrosymmetric. Therefore the central yttrium–hydroxo/oxo unit containing the yttrium, μ_3-OH, and terminal water molecules was taken to have two equally-weighted orientations related by the crystallographic inversion center. The model refined satisfactorily when these disordered atoms were set at half occupancy. Attempts to solve the structure assuming the alternative non-centrosymmetric space group $P1$ produced the same structure with the same kind of disorder. Therefore the centrosymmetric space group $P\bar{1}$ was retained for the final refinements. Further details of the crystal structure investigations for **1** may be obtained from the Fachinformationszentrum Karlsruhe, 76344 Eggenstein-Leopoldshafen, Germany (fax: (+49) 7247-808-666; e-mail: crysdata@fiz-karlsruhe.de) on quoting the depository number CSD-414282.

In both **1** and **2**, not all of the cationic counterions and the lattice water molecules could be located due, in part, to disorder. In addition, in **2**, the inherent difficulty in distinguishing NH_4^+ from H_2O in the electron-density difference maps also prevented their definitive assignment. Therefore, thermogravimetric and elemental analysis were used to determine the number of water molecules and countercations, respectively. CCDC-246002 contains the supplementary crystallographic data for **2**. This data can be obtained free of charge from the Cambridge Crystallographic Data Centre via www.ccdc.cam.ac.uk/data_request/cif.

Physical measurements: Infrared spectra (2% sample in KBr) were carried out on a Nicolet 510 FTIR instrument. Elemental analyses were performed by Kanti Labs in Mississauga, Canada. The ^{31}P NMR data were collected on a Varian Inova 400 MHz instrument with chemical shifts reported relative to 85% phosphoric acid. Spectral parameters: pulse width, 13 μs; delay, 5 s; sweep width, ±25000 Hz; acquisition time, 1.2 s. Typical sample concentrations were about 0.01 M. A polycrystalline powder of **Na2** was used to measure the magnetic properties. The magnetization data were determined using a static field of 1.0 and 10 kOe with a Cryogenic S600 SQUID magnetometer. The diamagnetic contribution of the sample holder was negligible (<0.1% of the signal) while the diamagnetic contribution of the compound was estimated using Pascal's constants.

Acknowledgement

We gratefully acknowledge the National Science Foundation (Grant CHE-0236686) for the research, and Grant CHE-9974864 for funding the D8 X-ray instrument. We thank Wade A. Neiwert and Kenneth I. Hardcastle for assistance with X-ray crystallography. We thank Professor Patrick Berthet at Université Paris-Sud, France, for assistance with the magnetic measurements.

[1] a) Z. Zheng, *Chem. Commun.* **2001**, 2521–2529, and references therein; b) Z. Zheng, R. Wang, *Comments Inorg. Chem.* **2000**, *22*, 1–30; c) J. W. Gilge, H. W. Roesky, *Chem. Rev.* **1994**, *94*, 895–910.

[2] a) N. Straeter, W. N. Lipscomb, T. Klabunde, B. Krebs, *Angew. Chem.* **1996**, *108*, 2158–2191; *Angew. Chem. Int. Ed. Engl.* **1996**, *35*, 2025–2055; b) J. Chin, *Curr. Opin. Chem. Biol.* **1997**, *1*, 514–521; c) J. Rammo, R. Hettich, A. Roigk, H.-J. Schneider, *Chem. Commun.* **1996**, *1*, 105–107.

[3] a) R. Wang, Z. Zheng, T. Jin, R. J. Staples, *Angew. Chem.* **1999**, *111*, 1929–1932; *Angew. Chem. Int. Ed.* **1999**, *38*, 1813–1815; b) B. Ma, D. Zhang, S. Gao, T. Jin, C. Yan, G. Xu, *Angew. Chem.* **2000**, *112*, 3790–3792; *Angew. Chem. Int. Ed.* **2000**, *39*, 3644–3646; c) B. Ma, D. Zhang, S. Gao, T. Jin, C. Yan, *New J. Chem.* **2000**, *24*, 251–252; d) R. Wang, H. Liu, M. D. Carducci, T. Jin, C. Zheng, Z. Zheng, *Inorg. Chem.* **2001**, *40*, 2743–2750; e) R. Wang, H. D. Selby, H. Liu, M. D. Carducci, T. Jin, Z. Zheng, J. W. Anthis, R. J. Staples, *Inorg. Chem.* **2002**, *41*, 278–286; f) J. C. Plakatouras, I. Baxter, M. B. Hursthouse, K. M. A. Malik, J. McAleese, S. R. Drake, *J. Chem. Soc. Chem. Commun.* **1994**, 2455–2456; g) X. Chen, Y. Wu, Y. Tong, Z. Sun, D. N. Hendrickson, *Polyhedron* **1997**, *16*, 4265–4272; h) W. J. Evans, M. A. Greci, J. W. Ziller, *Inorg. Chem.* **1998**, *37*, 5221–5226; i) R. Anwander, F. C. Munck, T. Priermeier, W. Scherer, O. Runte, W. A. Herrmann, *Inorg. Chem.* **1997**, *36*, 3545–3552.

[4] a) D. Kepert, *Inorganic Stereochemistry*, Springer, Berlin, **1982**; b) J.-C. G. Bünzli, *Basic and Applied Aspects of Rare Earths*, Editional Complutense, Madrid, **1997**.

[5] a) For recent reviews of POMs see: M. T. Pope, *Polyoxo Anions: Synthesis and Structure, Comprehensive Coordination Chemistry II*, *Vol. 4* (Ed.: A. G. Wedd), Elsevier Science, New York, **2004**, pp. 635–678; C. L. Hill, *Polyoxometalates: Reactivity, Comprehensive Coordination Chemistry II*, *Vol. 4* (Ed.: A. G. Wedd), Elsevier Science, New York, **2004**, pp. 679–759; b) A. J. Gaunt, I. May, D.

Collison, K. T. Holman, M. T. Pope, *J. Mol. Struct.* **2003**, *656*, 101–106.
[6] R. G. Finke, M. W. Droege, *Inorg. Chem.* **1983**, *22*, 1006–1008.
[7] R. G. Finke, M. W. Droege, P. J. Domaille, *Inorg. Chem.* **1987**, *26*, 3886–3896.
[8] T. J. R. Weakley, R. G. Finke, *Inorg. Chem.* **1990**, *29*, 1235–1241.
[9] C. J. Gómez-García, J. J. Borrás-Almenar, E. Coronado, L. Ouahab, *Inorg. Chem.* **1994**, *33*, 4016–4022.
[10] X. Zhang, Q. Chen, D. C. Duncan, C. F. Campana, C. L. Hill, *Inorg. Chem.* **1997**, *36*, 4208–4215.
[11] X. Zhang, T. M. Anderson, Q. Chen, C. L. Hill, *Inorg. Chem.* **2001**, *40*, 418–419.
[12] S. P. Harmalker, M. A. Leparulo, M. T. Pope, *J. Am. Chem. Soc.* **1983**, *105*, 4286–4292.
[13] R. G. Finke, B. Rapko, R. J. Saxton, P. J. Domaille, *J. Am. Chem. Soc.* **1986**, *108*, 2959.
[14] D. J. Edlund, R. J. Saxton, D. K. Lyon, R. G. Finke, *Organometallics* **1988**, *7*, 1692–1704.
[15] H. Weiner, J. D. Aiken, III, R. G. Finke, *Inorg. Chem.* **1996**, *35*, 7905–7913.
[16] E. Cadot, M.-A. Pilette, J. Marrot, F. Sécheresse, *Angew. Chem.* **2003**, *115*, 2223–2226; *Angew. Chem. Int. Ed.* **2003**, *42*, 2173–2176.
[17] a) U. Kortz, S. S. Hamzeh, N. A. Nasser, *Chem. Eur. J.* **2003**, *9*, 2945–2952; b) K. Nomiya, Y. Arai, Y. Shimizu, M. Takahashi, T. Takayama, H. Weiner, T. Nagata, J. A. Widegren, R. G. Finke, *Inorg. Chim. Acta* **2000**, *300–302*, 285–304.
[18] I. D. Brown, D. Altermatt, *Acta Crystallogr. Sect. B* **1985**, *41*, 244–247.
[19] The crystal radius of octahedrally coordinated W^{VI} is 0.72 Å, while those of eight-coordinate Yb^{III} and Y^{III} are 1.12 Å and 1.16 Å, respectively; R. D. Shannon, C. T. Prewitt, *Acta Crystallogr. Sect. B* **1969**, *25*, 925–946.
[20] J. Liu, E. A. Meyers, S. G. Shore, *Inorg. Chem.* **1998**, *37*, 5410–5411.
[21] a) J. Bartis, S. Sukal, M. Dankova, E. Kraft, R. Kronzon, M. Blumenstein, L. C. Francesconi, *J. Chem. Soc. Dalton Trans.* **1997**, 1937–1944; b) J. Bartis, M. Dankova, J. J. Lessmann, Q. Luo, W. D. Horrocks, Jr., L. C. Francesconi, *Inorg. Chem.* **1999**, *38*, 1042–1053.
[22] a) R. Contant, *Inorg. Synth.* **1990**, *27*, 106–111; b) B. J. Hornstein, R. G. Finke, *Inorg. Chem.* **2002**, *41*, 2720–2730.
[23] P.-H. Haumesser, R. Gaumé, B. Viana, E. Antic-Fidancev, D. Vivine, *J. Phys. Condens. Matter* **2001**, *13*, 5427–5447.
[24] E. Antic-Fidancev, J. Hölsä, M. Lastusaari, *J. Phys. Condens. Matter* **2003**, *15*, 863–876.
[25] a) N. Ishikawa, T. Iino, Y. Kaizu, *J. Am. Chem. Soc.* **2002**, *124*, 11 440–11 447; b) N. Ishikawa, M. Sugita, T. Okubo, N. Tanaka, T. Iino, Y. Kaizu, *Inorg. Chem.* **2003**, *42*, 2440–2446.
[26] Recently, Mialane and co-workers reported that an azido ligand plays a key role in the synthesis of a supramolecular tetradecanuclear copper polyoxometalate. See: P. Mialane, A. Dolbecq, J. Marrot, E. Rivière, F. Sécheresse, *Angew. Chem.* **2003**, *115*, 3647–3650; *Angew. Chem. Int. Ed.* **2003**, *42*, 3523–3526.
[27] a) J. Fuger, *Radiochim. Acta* **1992**, *59*, 81–91; b) J. I. Kim, *Mater. Res. Soc. Symp. Proc.* **1993**, *294*, 3–21.
[28] X. Fang, T. M. Anderson, W. A. Neiwert, C. L. Hill, *Inorg. Chem.* **2003**, *42*, 8600–8602.
[29] X. Fang, C. L. Hill, unpublished results.
[30] SMART Version 5.628, **2003**, Bruker AXS, Inc., Analytical X-ray Systems, 5465 East Cheryl Parkway, Madison WI 53711–5373, USA.
[31] SAINT Version 6.36 A, **2002**, Bruker AXS, Inc., Analytical X-ray Systems, 5465 East Cheryl Parkway, Madison WI 53711–5373, USA.
[32] SADABS Version 2.08, **2003**, George Sheldrick, University of Göttingen, Germany.
[33] SHELXTL Version 6.12, **2002**, Bruker AXS, Inc., Analytical X-ray Systems, 5465 East Cheryl Parkway, Madison WI 53711–5373, USA.
[34] *International Tables for X-ray Crystallography*, *Vol. C.* (Ed.: A. J. C. Wilson), Kluwer Academic, Dordrecht, **1992**, Tables 6.61.1.4 (pp. 500–502) and 4.2.6.8 (pp. 219–222).

Received: July 28, 2004
Published online: December 2, 2004